

This discussion paper is/has been under review for the journal Biogeosciences (BG).
Please refer to the corresponding final paper in BG if available.

Satellite detection of multi-decadal time series of cyanobacteria accumulations in the Baltic Sea

M. Kahru^{1,2} and R. Elmgren²

¹Scripps Institution of Oceanography, University of California San Diego, La Jolla, CA 92093-0218, USA

²Department of Ecology, Environment and Plant Sciences, Stockholm University, Stockholm, Sweden

Received: 26 January 2014 – Accepted: 18 February 2014 – Published: 26 February 2014

Correspondence to: M. Kahru (mkahru@ucsd.edu)

Published by Copernicus Publications on behalf of the European Geosciences Union.

BGD

11, 3319–3364, 2014

Cyanobacteria accumulations in the Baltic Sea

M. Kahru and R. Elmgren

Title Page

Abstract

Introduction

Conclusions

References

Tables

Figures

◀

▶

◀

▶

Back

Close

Full Screen / Esc

Printer-friendly Version

Interactive Discussion



Abstract

Cyanobacteria, primarily of the species *Nodularia spumigena*, form extensive surface accumulations in the Baltic Sea in July and August, ranging from diffuse flakes to dense surface scum. We describe the compilation of a 35 year (1979–2013) long time series of cyanobacteria surface accumulations in the Baltic Sea using multiple satellite sensors. This appears to be one of the longest satellite-based time series in biological oceanography. The satellite algorithm is based on increased remote sensing reflectance of the water in the red band, a measure of turbidity. Validation of the satellite algorithm using horizontal transects from a ship of opportunity showed the strongest relationship with phycocyanin fluorescence (an indicator of cyanobacteria), followed by turbidity and then by chlorophyll *a* fluorescence. The areal fraction with cyanobacteria accumulations (FCA) and the total accumulated area affected (TA) were used to characterize the intensity and extent of the accumulations. FCA was calculated as the ratio of the number of detected accumulations to the number of cloud free sea-surface views per pixel during the season (July–August). TA was calculated by adding the area of pixels where accumulations were detected at least once during the season. FCA and TA were correlated ($R^2 = 0.55$) and both showed large interannual and decadal-scale variations. The average FCA was significantly higher for the 2nd half of the time series (13.8 %, 1997–2013) than for the first half (8.6 %, 1979–1996). However, that does not seem to represent a long-term trend but decadal-scale oscillations. Cyanobacteria accumulations were common in the 1970s and early 1980s (FCA between 11–17 %), but rare (FCA below 4 %) from 1985 to 1990; they increased again from 1991 and particularly from 1999, reaching maxima in FCA (~ 25 %) and TA (~ 210 000 km²) in 2005 and 2008. After 2008 FCA declined to more moderate levels (6–17 %). The timing of the accumulations has become earlier in the season, at a mean rate of 0.6 days per year, resulting in approximately 20 days advancement during the study period. The interannual variations in FCA are positively correlated with the concentration of chloro-

BGD

11, 3319–3364, 2014

Cyanobacteria accumulations in the Baltic Sea

M. Kahru and R. Elmgren

Title Page

Abstract

Introduction

Conclusions

References

Tables

Figures

◀

▶

◀

▶

Back

Close

Full Screen / Esc

Printer-friendly Version

Interactive Discussion



phyll *a* in July–August sampled at the depth of ~ 5 m by a ship of opportunity program, but interannual variations in FCA are more pronounced.

1 Introduction

Surface or near-surface accumulations of cyanobacteria are common in the Baltic Sea during the summer months of July and August. They are caused by massive blooms of diazotrophic cyanobacteria, primarily *Nodularia spumigena* but also *Aphanizomenon* sp. that aggregate near the surface in calm weather (Öström, 1976; Kononen, 1992; Finni et al., 2001). Cyanobacteria blooms are considered a major environmental problem in the Baltic Sea because of the loss of recreational value of the sea and the beaches due to accumulations of foul-smelling, toxic cyanobacteria, and because their nitrogen fixation adds large amounts of potentially plant-available nitrogen to a eutrophicated and largely nitrogen-limited sea (Horstmann, 1975; Larsson et al., 2001). While the general factors enhancing cyanobacteria blooms such as availability of inorganic phosphorus, high surface temperature and strong near-surface stratification are well known, the specific factors determining the magnitude and distribution of the annual occurrence of these accumulations in different basins are still not understood and quantitative assessments and models allowing prediction of the accumulations are needed. Sediment records show that cyanobacteria blooms have occurred in the Baltic Sea for thousands of years (Bianchi et al., 2000). It is often assumed that their frequency and intensity have increased due to anthropogenic eutrophication (Horstmann, 1975), but such an increase has been difficult to demonstrate at the scale of the Baltic Sea, because of the intense patchiness and temporal variability of the blooms as well as due to the scarcity of reliable older measurements (Finni et al., 2001).

While the surface accumulations consist primarily of *Nodularia spumigena*, other species of cyanobacteria, primarily *Aphanizomenon* sp., often dominate in the water column (Hajdu et al., 2007; Rolff et al., 2007). These filamentous cyanobacteria have gas vacuoles that they can use to regulate their buoyancy (Walsby, 1994). These vac-

BGD

11, 3319–3364, 2014

Cyanobacteria accumulations in the Baltic Sea

M. Kahru and R. Elmgren

Title Page

Abstract

Introduction

Conclusions

References

Tables

Figures

◀

▶

◀

▶

Back

Close

Full Screen / Esc

Printer-friendly Version

Interactive Discussion



ules are very effective backscatterers of visible light (Volten et al., 1998) and are the major contributor to the brightness that makes the accumulations visible in satellite images (Fig. 1).

Due to their temporal and spatial variability (“patchiness”), cyanobacteria surface accumulations are extremely difficult to monitor using ship-based sampling (Kutser, 2004). Their concentrations often vary by more than 2 orders of magnitude over the distance of a few meters and no suitable quantitative methods are available for reliable ground-truth measurements. Satellites sensors allow synoptic view over large spatial domains but visible and near-infrared sensors are limited to cloud-free periods. Automated shipborne measurements of phycocyanin fluorescence (Seppälä et al., 2007) and hyperspectral reflectance (Simis and Olsson, 2013) have the potential to provide ground-truth measurements even under cloudy conditions, but are restricted to limited horizontal transects along shipping routes. The first satellite images of the Baltic Sea showing *Nodularia* accumulations were acquired by Landsat MSS in 1975 (Öström, 1976; Horstmann, 1983). However, due to the narrow swath width and low sampling frequency the Landsat sensors produced only a few scenes per year for the whole Baltic which was insufficient for creating quantitative time series. A problem affecting all satellite data has been the lack of quantitative algorithms for estimating cyanobacteria concentrations as no suitable standard satellite products are available. The first quantitative satellite-based time series using the broad-band weather sensor AVHRR was created in the 1990s (Kahru et al., 1994) but AVHRR data had problems separating cyanobacteria from other forms of turbidity or high surface reflectance. More sophisticated spectral methods that are specific to the pigment composition and other optical characteristics of cyanobacteria have been proposed (e.g. Matthews et al., 2012) but are specific to a particular set of spectral bands, e.g. those on the MERIS sensor that operated in 2003–2012. A time series based on only MERIS data would be too short to reveal multi-decadal variability. Time series become more valuable, the longer they get, making it essential to be able to merge data from multiple satellite sensors. We have developed simple algorithms that can be applied to various satellite sensors from the

BGD

11, 3319–3364, 2014

Cyanobacteria accumulations in the Baltic Sea

M. Kahru and R. Elmgren

Title Page

Abstract

Introduction

Conclusions

References

Tables

Figures



Back

Close

Full Screen / Esc

Printer-friendly Version

Interactive Discussion



wide-band (~ 100 nm) and low signal-to-noise ratio (SNR) AVHRR sensor to modern ocean color sensors with spectrally narrow (~ 10 nm) bands and high SNR. Using these algorithms we have compiled a quantitative time series of cyanobacteria accumulation characteristics in the Baltic Sea since 1979.

2 Data and methods

2.1 Satellite data

A summary of the various satellite sensors that have been used to detect cyanobacteria from space is in Table 1. The first ocean color sensor CZCS (Hovis et al., 1980) was an experimental sensor operated by NASA from 1978 to 1986 and was turned on only intermittently due to its limited recording capacity. A reasonable number of CZCS scenes from the Baltic Sea are available for the July–August season from 1979 to 1984 (Table 2). CZCS data were downloaded as Level-2 files from NASA's ocean color web (<http://oceancolor.gsfc.nasa.gov/>).

A broad-band weather sensor, named Advanced Very High Resolution Radiometer (AVHRR), has been flown on a series of NOAA polar orbiting satellites and data are available since 1979 (Kidwell, 1995). The advantages of AVHRR are its wide swath (over 2000 km), frequent coverage (up to several passes per day), and availability over a long period of time. However, compared to specialized ocean color sensors, AVHRR has only two broadband spectral channels in the visible (0.58–0.68 μm) and near infrared (0.72–1.10 μm) with low sensitivity and poor calibration accuracy. This makes atmospheric correction difficult and limits its capability to distinguish algal blooms near and at the surface from suspended sediments, certain types of clouds as well as bottom reflection in shallow areas. In spite of these limitations, AVHRR data has been used to detect bright blooms such as coccolithophores (Groom and Holligan, 1987) and cyanobacteria in the Baltic (Kahru et al., 1993, 1994, 2000; Kahru, 1997). We used AVHRR data recorded at multiple locations, including Stockholm University. The

BGD

11, 3319–3364, 2014

Cyanobacteria accumulations in the Baltic Sea

M. Kahru and R. Elmgren

Title Page

Abstract

Introduction

Conclusions

References

Tables

Figures

⏪

⏩

◀

▶

Back

Close

Full Screen / Esc

Printer-friendly Version

Interactive Discussion



Cyanobacteria accumulations in the Baltic Sea

M. Kahru and R. Elmgren

Title Page

Abstract

Introduction

Conclusions

References

Tables

Figures



Back

Close

Full Screen / Esc

Printer-friendly Version

Interactive Discussion



most complete archive of AVHRR over Europe since 1979 is available from the Dundee Satellite Receiving Station (<http://www.sat.dundee.ac.uk/>). For detecting cyanobacteria we used only satellite passes near local noon (10:00–14:00 LT), as atmospheric scattering and absorption mask the relatively weak signal from the water surface at low sun elevation. While data from AVHRR sensors were transmitted daily, due to various failures we have less than the maximum number of daily AVHRR datasets during the July–August period of the early years (Table 3).

Data from modern ocean color sensors are available daily with multiple passes per day and all Level-2 data files from SeaWiFS, MODIS-Aqua (MODISA), MODIS-Terra (MODIST) and VIIRS sensors of the summer months from June to August were downloaded from NASA's ocean color archive (<http://oceancolor.gsfc.nasa.gov/>). The total number of files (Table 4) depends on the number and type of sensors. SeaWiFS was the only ocean color sensor operational in 1998–1999. After that period (2000 and later) data from multiple ocean color sensors were available simultaneously (Table 5). SeaWiFS Level-2 datasets are distributed in a single file whereas MODISA, MODIST and VIIRS data are broken into multiple granules and therefore the number of files is higher. Between 2005 and 2010 SeaWiFS data were only available at the low (4 km) resolution (GAC) mode and were not used. We combine multiple satellite passes and multiple files per day and show the number of days in July–August with useable data (“N of valid days”) in Table 5. Scenes that were completely cloudy or produced no valid data of the water surface were excluded.

All satellite data were registered to a standard equal area map in Albers conic projection with 1 km² pixel size (Fig. 2). Since cyanobacteria blooms are not known to occur in the Bothnian Bay, this northernmost part of the Baltic Sea was excluded from all maps and calculations. Coastal zones and other turbid areas were also excluded (more below).

While we have better data coverage from 1998 and onwards (Fig. 3), even the approximately 40–50 days of combined AVHRR and CZCS coverage in the early years of 1979 to 1986 are sufficient for quantitative seasonal estimates as the accumulations

are relatively consistent from day to day. The detected total area approaches a plateau after about one satellite image per bloom day (Fig. 3.9 in Kahru, 1997) and the fraction of cyanobacteria accumulations (details below) are normalized to the number of clear (valid) viewings.

2.2 Methods of detecting cyanobacteria accumulations

2.2.1 AVHRR

The low sensitivity and poor calibration accuracy of AVHRR's two broadband spectral channels make accurate atmospheric correction difficult. Even with the best available calibration coefficients, atmospheric correction often resulted in physically impossible negative values of the water-leaving radiance (Stumpf and Fryer, 1997). We therefore used the standard AVHRR band 1 albedo (Kidwell, 1995) to detect cyanobacteria. The supervised classification algorithm as applied to AVHRR data has been described previously (Kahru et al., 1994; Kahru, 1997). The range of band 1 albedo of the accumulations was determined empirically and varied between 2.3 % and 4 %, with lower values classified as water and higher values as clouds. However, these values were used as guidance and had to be empirically adjusted for some scenes. The surface distribution of cyanobacteria accumulations has a very characteristic spatial texture and patterns of swirls, eddies and filaments (Fig. 1) that are useful in separating the accumulations from clouds, fog and aircraft contrails. Areas with such high spatial texture were considered cyanobacteria accumulations. Multiple thresholdings and differences in the visible, near infrared and thermal channels were used to eliminate pixel areas with similar albedo. Data in the near infrared band 2 and the two thermal infrared bands, 4 (10.4–11.0 μm) and 5 (11.6–12.2 μm), were used to screen clouds, haze, land and error pixels. Pixels with band 2 albedo values exceeding the corresponding band 1 albedo by 0.2 % were classified as land or considered an error. Pixels with band 4 and band 5 difference greater than 2 °C were designated as clouds. Finally, visual inspection and editing were used to eliminate pixels erroneously marked as accumulations due to variable clouds

Cyanobacteria accumulations in the Baltic Sea

M. Kahru and R. Elmgren

Title Page

Abstract

Introduction

Conclusions

References

Tables

Figures



Back

Close

Full Screen / Esc

Printer-friendly Version

Interactive Discussion



Cyanobacteria accumulations in the Baltic Sea

M. Kahru and R. Elmgren

Title Page

Abstract

Introduction

Conclusions

References

Tables

Figures



Back

Close

Full Screen / Esc

Printer-friendly Version

Interactive Discussion



and sediment-rich coastal areas. As cyanobacteria accumulations are usually present in the same location for more than one day, while clouds and other atmospheric effects are more transient, sequences of images were checked for consistency of the detected accumulations over several images and suspected classification errors were manually deleted. When some of the AVHRR data were reprocessed in 2012–2013 to compare with modern ocean color data, some of the tests were skipped and valid ocean areas were determined as channel 1 albedo less than 4 % and the cyanobacteria accumulations were determined visually by their high reflectance and characteristic spatial patterns. While these methods cannot unequivocally separate isolated accumulations from certain thin clouds, floating pine pollen or suspended sediments in shallow areas or near the coast, large-scale cyanobacteria accumulations, particularly those of *Nodularia*, mainly occur offshore (e.g., Wasmund, 1997), away from the coast and are clearly detected. Near-shore areas with depth less than 30 m and frequent turbidity were eliminated using a fixed map (Fig. 2) as reliable separation of accumulations from other forms of turbidity was not possible in coastal areas. A sample AVHRR image showing extensive cyanobacteria accumulations in band 1 albedo and the corresponding maps of detected accumulations as well as valid ocean area are shown in Fig. 4. A comparison of detecting the same accumulations (10 July or 11 July 2005) with the more accurate ocean color imagery (MODIS-Aqua and MODIS-Terra) is shown in Figs. 5 and 6.

2.2.2 Ocean color sensors

The methods applied to modern ocean color sensors such as SeaWiFS, MODISA, MODIST and VIIRS as well as the early CZCS were essentially the same as described in Kahru et al. (2007). After the 2009 reprocessing, the standard NASA ocean color output is remote sensing reflectance (Rrs) instead of the formerly used normalized water leaving radiance (nLw). The conversion between Rrs and nLw is straightforward: $nLw(\lambda) = \text{solar_irradiance}(\lambda) \times Rrs(\lambda)$. The semi-automated method of detection of cyanobacteria accumulations is based on visually evaluating images of $Rrs555$

(SeaWiFS) or *Rrs547* (MODISA and MODIST) or *Rrs551* (VIIRS) and automatically thresholding *Rrs* of the approximately 670 nm band (*Rrs667* for MODISA and MODIST, *Rrs670* for SeaWiFS, *Rrs671* for VIIRS) for turbidity. High reflectance in the 670 nm band is caused by strong backscattering of particles that are either in the water column near the surface or directly at the surface (surface scum). Both near-surface and surface backscattering is indicative of high cyanobacteria concentrations. High water reflectance at 670 nm can also be caused by various other particles in the water column, i.e. turbidity, such as organic and inorganic particles in river runoff or re-suspended particles from the bottom or other particles floating at the surface (such as pine pollen). However, such other causes of turbidity or high backscattering are rare in the open Baltic Sea in July and August. Thresholding of the *Rrs* of the red band is part of the standard NASA level-2 processing and the Level-2 flag TURBIDW (“turbid water”) is set if $Rrs670 > 0.012 \text{ sr}^{-1}$ (<http://oceancolor.gsfc.nasa.gov/VALIDATION/flags.html>). For detecting cyanobacteria accumulations we also require that the flag MAXAERITER (maximum aerosol iteration) is off as this flag is set if there is a problem in atmospheric correction that often occurs near cloud edges. Using the MAXAERITER flag eliminates many false positives. A pixel is classified as a valid ocean pixel only if none of the following flags are set: ATMFAIL, LAND, HIGLINT, HILT, HISATZEN, STRAYLIGHT, CLDICE, HISOLZEN, LOWLW, CHLFAIL, MAXAERITER, ATMWARN. The primary flag here is CLDICE that indicates high reflectance due to clouds, as ice is not possible in the July–August imagery. The flag COASTZ is not used. A pixel is classified as an accumulation if (1) it is a valid ocean pixel and (2) if it has the high turbidity flag set. Near-shore and shallow areas of known high reflectance due to river runoff and resuspended sediments are excluded (Fig. 2). Atmospheric correction failure sometimes occurred in the middle of the densest cyanobacteria accumulations and was caused by dense surface scum. These areas in the middle of accumulations were clearly identifiable and were manually filled with the turbid water class. They always represented a small (< 5 %) fraction of the total area of detected accumulations. Some manual elimination of false positives was needed for SeaWiFS data, particularly along cloud edges. SeaWiFS data have lower

Cyanobacteria accumulations in the Baltic Sea

M. Kahru and R. Elmgren

Title Page

Abstract

Introduction

Conclusions

References

Tables

Figures



Back

Close

Full Screen / Esc

Printer-friendly Version

Interactive Discussion



sensitivity than MODIS data and therefore higher levels of noise variance (Hu et al., 2013). Some areas, e.g. the Gulf of Riga, are almost always turbid and the detection of cyanobacteria accumulations there is ambiguous. In these areas accumulations were confirmed only if the adjacent areas also showed accumulations.

5 A comparison of the results of applying the algorithms to 10–11 July 2005 imagery of MODISA and MODIST (Figs. 5 and 6) shows good agreement between those two as well as AVHRR (Fig. 4).

The CZCS is less sensitive than SeaWiFS and MODIS and the TURBIDW flag is almost never set for valid ocean pixels. We therefore used the high reflectance determined as $nLw555 > 0.8 \text{ mW cm}^{-2} \mu\text{m}^{-1} \text{ sr}^{-1}$ with characteristic spatial patterns to detect likely cyanobacteria accumulations.

2.3 Routine processing of satellite data

Multiple satellite passes (Level-2 unmapped datasets) that were classified into valid ocean and turbid classes were registered to a standard map in Albers conic equal area projection with a 1 km^2 pixel size (Fig. 2) and composited into daily maps of valid ocean and turbid ocean classes. Those daily maps from individual satellite sensors were then composited into merged daily maps of valid and turbid classes, respectively. For each pixel the counts of valid and turbid classes were accumulated over 5 days, one month and 2 month periods. From these counts the fraction of cyanobacteria accumulations (FCA) was calculated as the ratio of the number of counts: $N(\text{turbid})/N(\text{valid})$. FCA shows the fraction of days when cyanobacteria accumulation was detected per cloud-free daily measurements. Another metric that has been used in the past, the total area (TA) or cumulative area, shows the total area where accumulations were detected at least once during the whole season (June to August). As the area of each pixel in our standard map is 1 km^2 , TA in km^2 is equivalent to the number of detected turbid pixels in the overall (seasonal) composite of turbid areas. *Nodularia* blooms producing surface accumulations typically occur from the end of June to the end of August (Kononen, 1992; Kahru et al., 1994; Wasmund, 1997). The monthly mean FCA for June is normally

Cyanobacteria accumulations in the Baltic Sea

M. Kahru and R. Elmgren

Title Page

Abstract

Introduction

Conclusions

References

Tables

Figures



Back

Close

Full Screen / Esc

Printer-friendly Version

Interactive Discussion



very low. We therefore used the July to August mean FCA as the indicator of the annual intensity of the accumulations.

A total of 1990 daily datasets (Table 5), typically merged from multiple sensors, were used over the July–August period of 1979–2013 which makes an average of over 57 days per year (out of the maximum of 62 days per July–August). The number of individual scenes per day could be further increased by using the 10 year of MERIS data (2002–2011 for the July–August period) and the full-resolution SeaWiFS data for 2005–2010. However, these data will not increase the number of daily valid datasets as these years are already well covered by other sensors.

2.4 Comparison between the outputs of different sensors

Satellite sensors differ in overpass times, orbits and swath widths, view and solar angles, as well as spectral bands and sensitivities (e.g. signal-to-noise ratio, SNR). Their sensitivity can change over time and NASA therefore continuously monitors, and intermittently recalibrates and reprocesses all previously collected data. Variations between FCA of different sensors are therefore to be expected, particularly due to differences in overpass times and in the surface areas obscured by clouds. In order to evaluate the errors and variability of our FCA estimates we compared the mean monthly FCAs obtained by multiple simultaneous sensors in 9 different areas of the Baltic Sea (Fig. 2). Larger random variations are expected for smaller areas, e.g. the Bay of Gdansk.

SeaWiFS, MODIST, MODISA and VIIRS have all overlapped temporally with at least one other sensor. We used FCA obtained from MODIST (FCA_T) as the common ordinate variable in comparisons with all other sensors (Fig. 7). The results showed that FCA values obtained with temporally overlapping ocean color sensors (SeaWiFS, MODIST, MODISA and VIIRS) were all highly correlated ($R^2 \sim 0.94\text{--}0.96$) and had a linear regression with an intercept that was not significantly different from zero and a slope that was close to 1.0. These conclusions were also confirmed separately for individual years when FCA could be compared for two sensors. The only exception was year 2011 when FCA_T was approximately 1.3 times higher than FCA ob-

Cyanobacteria accumulations in the Baltic Sea

M. Kahru and R. Elmgren

Title Page

Abstract

Introduction

Conclusions

References

Tables

Figures



Back

Close

Full Screen / Esc

Printer-friendly Version

Interactive Discussion



Cyanobacteria accumulations in the Baltic Sea

M. Kahru and R. Elmgren

[Title Page](#)

[Abstract](#)

[Introduction](#)

[Conclusions](#)

[References](#)

[Tables](#)

[Figures](#)



[Back](#)

[Close](#)

[Full Screen / Esc](#)

[Printer-friendly Version](#)

[Interactive Discussion](#)



tained with MODISA ($FCA_T = 1.316 \times FCA_A + 0.0015$, $R^2 = 0.9413$, $N = 27$). The reason for this anomaly is not clear but it is possible that the slightly higher FCA_T was caused by the higher noise level and less accurate calibration of MODIST. Another factor that may influence the difference between sensors is the overpass time. The MODIS-Terra overpass was at approximately 10:30 LT and the MODIS-Aqua overpass at approximately 13:30 LT. During calm weather it might be expected that more accumulations would develop by the afternoon, but currently we have not confirmed any systematic influence of the overpass time on FCA. FCA derived with the new VIIRS sensor corresponds well to FCA derived with the other sensors for the two years (2012 and 2013) available for comparison (Fig. 7c).

The error of the monthly FCA as determined by a satellite sensor can be estimated as (1) the mean absolute difference and (2) the median absolute difference between FCA values of different sensors. For MODISA, MODIST and VIIRS the mean absolute differences were from 1.1 to 1.9% FCA and the median absolute differences were between 0.4 and 0.6% FCA. For SeaWiFS the respective errors were slightly higher (2.0% and 1.1% FCA, respectively).

Considering the highly variable nature of the accumulations and the variable orbits covering the Baltic Sea at different times of the day, we concluded that the differences between FCA values obtained by different ocean color sensors were insignificant and therefore the results of individual sensors could be merged to estimate FCA.

Larger differences in FCA are expected when comparing the “new” ocean color sensors with the “old” and less accurate AVHRR sensor. Due to its lower sensitivity, AVHRR is expected to be less effective in detecting accumulations that are small or barely above the detection limit of the more sensitive ocean color sensors. We compared FCAs from the AVHRR on NOAA satellites (FCA_N) with FCAs from SeaWiFS (1998, 1998), MODISA (2005) and MODIST (2000, 2005) in 9 areas of the Baltic in July and August. The overall linear regression between FCA_N and FCA has an R^2 of 0.82, which increased to 0.94 when excluding the often turbid areas of Gdansk Bay, Gulf of Riga and eastern Gulf of Finland where detection is often ambiguous. An un-

derestimation by FCA_N is particularly evident at low FCA levels. We approximated this relationship with a power function $FCA_N = 0.95 \times FCA^{1.5}$ which models the lower detection efficiency at low FCA and the relatively good detection efficiency at high FCA. It appeared that the dense and large-scale accumulations were well detected by AVHRR and produced FCA values that are only slightly lower than FCAs determined simultaneously with ocean color sensors (Fig. 7d). We then used the inversion of the power function to convert FCA_N to FCA. We concluded that after applying the conversion, FCA determined with AVHRR was comparable to FCA determined with other sensors, particularly for the intense and large-scale accumulations that mattered most in detecting the interannual variability.

2.5 Horizontal transects measured on ships of opportunity

For validating the daily images of satellite-detected cyanobacteria accumulations we used horizontal transects obtained from the Algaline (Rantajärvi, 2003) ships of opportunity instrumented with a system measuring, among others, chlorophyll *a* (Chl*a*) fluorescence, phycocyanin (PC) fluorescence and turbidity (Seppälä et al., 2007). The flow-through instrument system was installed on a ferryboat commuting between Helsinki (Finland) and Travemünde (Germany) and sampled from flow-through water pumped from approximately 5 m depth. For this analysis we used data collected during 15 transects in July 2010 and provided by J. Seppälä (Finnish Environment Institute, SYKE). The measured relative voltages of PC fluorescence, Chl*a* fluorescence and turbidity were normalized between the respective minimums and maxima and converted to a scale from 0 to 100. For each ship measurement the nearest satellite pixel was found in the corresponding daily merged image of detected accumulations and valid pixels were averaged in the 5×5 pixel neighborhood centered at the nearest satellite pixel. A pixel with detected accumulation was assumed to have a value of 1 and a valid pixel with no detected accumulation to have a value of 0. This averaging was performed to compensate for the navigation errors and for the possible advection of the accumula-

BGD

11, 3319–3364, 2014

Cyanobacteria accumulations in the Baltic Sea

M. Kahru and R. Elmgren

Title Page

Abstract

Introduction

Conclusions

References

Tables

Figures

◀

▶

◀

▶

Back

Close

Full Screen / Esc

Printer-friendly Version

Interactive Discussion



tions during the temporal shift between satellite passes and ship measurements (up to 24 h).

3 Results

3.1 Validation of satellite detection of cyanobacteria accumulations with horizontal transects measured on ships of opportunity

Figure 8 shows a comparison between four ship transects of phycocyanin (PC) fluorescence and satellite detection of cyanobacteria accumulations on single day images in July 2010. The accumulations started to be detectable in the beginning of July in the Bay of Gdansk (near 19° E longitude) and were accurately detected by the satellite algorithm (Fig. 8a and b). By 10 July the accumulations were widespread both in the Northern and Southern Baltic Proper (Fig. 8c and d). The narrow tongue of accumulations just outside of the Bay of Gdansk was well detected by both measurements. In the southwestern Baltic the band of increased PC fluorescence (14–15° E) was associated with a few scattered detected pixels of accumulations and the corresponding average cyanobacteria score was therefore relatively low. On 12 and 20 July massive accumulations covered both Northern and Southern Baltic Proper but the ship track was not optimal for detecting particularly the southern accumulations. The ship transects on 12 July (west of the island of Gotland, Fig. 8e and f) and on 20 July (east of Gotland, Fig. 8g and h) were both along the edge of the major area of accumulations in the Southern Baltic Proper and that probably caused a large part of the variability in the average cyanobacteria score there. Narrow strips of increased PC fluorescence corresponded well to detected cyanobacteria but we could not detect a common threshold of PC fluorescence above which the surface accumulations could be detected by our satellite algorithm. That was expected as the correspondence between ship measurements at 5 m depth and satellite measurements of the surface layer depends on the vertical distribution of cyanobacteria and the depth of the top layer within which the

BGD

11, 3319–3364, 2014

Cyanobacteria accumulations in the Baltic Sea

M. Kahru and R. Elmgren

Title Page

Abstract

Introduction

Conclusions

References

Tables

Figures



Back

Close

Full Screen / Esc

Printer-friendly Version

Interactive Discussion



cyanobacteria flakes (aggregates of filaments) are distributed. As our output variable was binary (1 = accumulations detected; 0 = accumulations not detected), we used the logistic regression to model the relationship between predictor variables such as PC fluorescence, Chla fluorescence or turbidity and the binary response variable. Best fits of the 2 parameters, intercept (a) and slope (b), were searched for the following equation:

$$P = \frac{1}{1 + e^{-(a+bX)}} \quad (1)$$

We used the Newton–Raphson method of iteratively finding the best fit as implemented in the NMath numerical libraries (<http://www.centerspace.net/>). As in linear regression, we were interested in finding the best model of a predictor variable to help explain the binary output. It turned out that all three predictor variables were significantly related to the detected cyanobacteria but the strongest relationship was with PC fluorescence, followed by turbidity and then by Chla fluorescence. All estimates of the goodness of fit (G-statistic, Pearson statistic, Hosmer Lemeshow statistic) showed significant relationships at the 0.05 level of significance. The parameters of the logistic regression were not constant from transect to transect. That was expected as the voltages were not calibrated in absolute concentrations but mostly due to the variable relationships between surface-detected accumulations and the vertical distribution of cyanobacteria in the water column (Groetsch et al., 2012). For a typical transect (15 July 2010) the logistic regression parameters with PC fluorescence were: intercept 2.79 (0.05 confidence interval to 2.61 to 2.96), slope 0.083 (0.05 confidence interval 0.076 to 0.090). Probability curves of the accumulations for the full ranges of predictor variables (Fig. 9) show that detected cyanobacteria accumulations were most sensitive to PC fluorescence and somewhat less to turbidity. The effect of Chla fluorescence had a much weaker effect and the relationship was less tight.

Cyanobacteria accumulations in the Baltic Sea

M. Kahru and R. Elmgren

[Title Page](#)[Abstract](#)[Introduction](#)[Conclusions](#)[References](#)[Tables](#)[Figures](#)[Back](#)[Close](#)[Full Screen / Esc](#)[Printer-friendly Version](#)[Interactive Discussion](#)

3.2 Timing of the accumulations

Figure 10 shows the monthly FCA of the months of June, July and August for the period when most accurate coverage exists (from 1998 to 2012). While the first accumulations often appear in June, the mean monthly FCA for June is always very low. In some years (2002, 2003, 2005, 2006, 2008, 2010 and 2013) the July FCA is much higher than that of August whereas in other years (1998, 2007, 2011 and 2012) July and August have similar FCA. The highest FCAs were recorded in periods of warm and sunny weather. As the monthly period of compositing is too long to discover smaller temporal changes, we made 5 day composited FCA for each pixel. In analogy with the calculation of the center of gravity, we calculated the “center of timing”. For each year and each pixel we estimated $G = \sum(\text{day} \times \text{FCA})$ and $F = \sum \text{FCA}$ where day is the middle year-day of the 5 day period and FCA is the 5 day FCA of a pixel. The center of timing was defined as G/F and represents the temporal center of the accumulations in year-days. For an individual pixel the annual center of timing can be quite variable. We therefore used the median for a larger area of pixels, e.g. the whole Baltic Sea or any of the 9 sub-areas (Fig. 2). Figure 11a shows the median of the center of timing for the whole Baltic Sea from 1979 to 2013. In spite of the strong interannual variability a significant ($P < 0.001$) trend towards earlier occurrence can be detected. The mean trend is approximately 0.6 days per year or 6 days per decade. This means that over the 35 year observation period the center of timing in the Baltic Sea has become 20 days earlier. The mean center of timing has therefore changed from approximately 8 August (year-day 220) to 19 July (year-day 200). The trend in center of timing can be estimated also in each of the 9 sub-areas but the interpretation is less obvious as some years may not have any accumulations. The Northern Baltic Proper and the Eastern Gotland Basin (sub-areas 4 and 6) are the only sub-areas with at least some accumulations for the whole 35 year period and the trend towards earlier occurrence is also visible there (Fig. 11b). The interannual variations in the timing of the accumulations in individual areas are typically coherent over the whole Baltic Sea. Accumulations in the Bothnian Sea typically occur

BGD

11, 3319–3364, 2014

Cyanobacteria accumulations in the Baltic Sea

M. Kahru and R. Elmgren

Title Page

Abstract

Introduction

Conclusions

References

Tables

Figures



Back

Close

Full Screen / Esc

Printer-friendly Version

Interactive Discussion



Cyanobacteria accumulations in the Baltic Sea

M. Kahru and R. Elmgren

[Title Page](#)

[Abstract](#)

[Introduction](#)

[Conclusions](#)

[References](#)

[Tables](#)

[Figures](#)

[⏪](#)

[⏩](#)

[◀](#)

[▶](#)

[Back](#)

[Close](#)

[Full Screen / Esc](#)

[Printer-friendly Version](#)

[Interactive Discussion](#)



tative interannual time series of sufficient length. In the era of anthropogenic climate change it is common and justified to look for trends in environmental variables but the observed changes in relatively short time series are most often due to decadal or interannual variability rather than to secular trends. In order to build time series that are as long as possible, we used multiple satellite sensors and included both the “old” and “new” datasets.

Several algorithms using spectral bands in the red and the “red edge” portion of the near-infrared spectrum can be applied to MERIS data for the detection of cyanobacteria, e.g. the fluorescent line height (FLH, Gower et al., 1999), the maximum chlorophyll index (MCI, Gower et al., 2006), the cyanobacteria index (CI, Wynne et al., 2008) and the Maximum Peak Height (MPH, Matthews et al., 2012). Hyperspectral sensors, e.g. HICO (Lucke et al., 2011), have even more potential in creating algorithms that are specific to particular features in the absorption, fluorescence or backscattering spectra of cyanobacteria. While these algorithms are potentially more accurate for separating cyanobacteria from other types of algae and other substances in the water, they are specific to the band sets of particular sensors (e.g. MERIS). Therefore those algorithms cannot be extended backwards to the early sensors. We therefore did not attempt to use these spectral methods of detecting cyanobacteria. An important factor in the application of these spectral algorithms is that the optical characteristics of cyanobacteria accumulations are very sensitive to their vertical distribution. As water absorbs strongly in the red part of the spectrum, it makes a drastic difference to the reflectance spectrum if the accumulations extend slightly above the water surface (i.e. surface scum) or are submerged just under the air–water interface. A sudden increase in wind speed can quickly change the vertical structure of the accumulations, mix the accumulations in the upper few meters and drastically change the output of algorithms that are too sensitive to the vertical distribution of the accumulations. For example, the normalized vegetation index (NDVI) that is being used to detect land vegetation can be applied to the Baltic AVHRR data (Kahru et al., 1993) but it detects only the surface scum that can disappear and reappear within a day depending on the wind speed. Multi- and

hyper-spectral algorithms are not applicable to old sensors like AVHRR with only one band in the visible part of the spectrum. In order to create a series as long as possible using different kinds of satellite sensors including those with low signal-to-noise ratio, we opted to use simple, generic algorithms that are sensitive to brightness in the red part of the spectrum.

It is technically challenging to create a consistent time series that combines data from multiple satellite sensors over a long time period. We have here provided methods for linking estimates of FCA from the “old” AVHRR and CZCS sensors with those from the “new” ocean color sensors, and created a 35 year long time series of the frequency of cyanobacteria accumulations in the Baltic Sea. While our satellite data are limited to cloud-free periods and detect the presence cyanobacteria only by their surface signature, the relative temporal consistency of the accumulations and the large number of satellite measurements (Table 4) gives us confidence in the interannual time series. It is difficult to compare our interannual time series with the results from the traditional monitoring programs which typically sample a few fixed stations once per month. A single monthly sample can easily miss the high cyanobacteria concentration in a plume floating nearby (e.g. Finni et al., 2001) and the mean error for the more stable chlorophyll *a* concentration has been estimated to be ~ 100 % due to temporal aliasing and another ~ 100 % due spatial heterogeneity (Kahru and Aitsam, 1985). Higher temporal and spatial frequency is provided by programs like Algaline (Ranta-järvi, 2003) using ships of opportunity. However, the Chla *in vivo* fluorescence that is often used as a measure of phytoplankton biomass is a poor measure of the abundance of cyanobacteria as most of the cyanobacterial Chla is located in the non-fluorescing photosystem I (Seppälä et al., 2007 and references therein). It was also confirmed in this work that Chla fluorescence was a worse predictor for detecting cyanobacteria accumulations than either phycocyanin fluorescence or turbidity (Fig. 9). The Algaline program also collects a small number discrete water samples that are used to measure Chla from extracts using standard methods. The extracted Chla is much better correlated with cyanobacteria abundance (Seppälä et al., 2007) than Chla fluorescence.

Cyanobacteria accumulations in the Baltic Sea

M. Kahru and R. Elmgren

[Title Page](#)[Abstract](#)[Introduction](#)[Conclusions](#)[References](#)[Tables](#)[Figures](#)[Back](#)[Close](#)[Full Screen / Esc](#)[Printer-friendly Version](#)[Interactive Discussion](#)

Cyanobacteria accumulations in the Baltic Sea

M. Kahru and R. Elmgren

Title Page

Abstract

Introduction

Conclusions

References

Tables

Figures



Back

Close

Full Screen / Esc

Printer-friendly Version

Interactive Discussion



Preliminary comparison between Chla values extracted from discrete water samples provided by S. Kaitala (Finnish Environment Institute, SYKE) and FCA along the ship tracks where samples were collected showed quite similar interannual patterns. The mean chlorophyll *a* concentration of samples collected in July–August in the Eastern Gotland basin had a coherent pattern with FCA ($R = 0.69$, Fig. 15) but much lower variability (mean = 3.8 mg m^{-3} , coefficient of variation = 0.22). The corresponding time series of FCA had a coefficient of variation that was 4–5 times higher (1.03 for 1995–2012 and 1.34 for 1979–2013). This difference in variability was expected as Chla integrates all phytoplankton whereas FCA is a much more sensitive parameter as the detection of surface accumulations requires very high concentrations of cyanobacteria (primarily *Nodularia*) near the surface. An analysis of the environmental conditions explaining the interannual patterns in FCA (cf. Kahru et al., 2007) is planned for the future. Future work should also compare this FCA dataset with the more advanced multi- and hyperspectral methods like the Maximum Peak Height (Matthews et al., 2012).

Acknowledgements. Financial support was provided to R. E. by the Swedish Research Council Formas and the Stockholm University's Baltic Ecosystem Adaptive Management Program. Satellite ocean color data were provided by the NASA Ocean Color Processing Group. AVHRR data were provided by Dundee Satellite Receiving Station. The authors thank S. Kaitala for providing Algaline extracted chlorophyll *a* data, J. Seppälä for providing the Algaline transect data, T. Tamminen and Oleg Savchuk for useful discussions and Andrew Brooks for AVHRR data conversion.

References

- Apstein, C.: Das Plankton der Ostsee (Holsatia Expedition 1901), Abhandl. Deutschen Seefischerei-Vereins, VII, 103–129, 1902 (In German).
- Bianchi, T. S., Engelhaupt, E., Westman, P., Andren, T., Rolff, C., and Elmgren, R.: Cyanobacterial blooms in the Baltic Sea: natural or human-induced?, *Limnol. Oceanogr.*, 45, 716–726, 2000.

Cyanobacteria accumulations in the Baltic Sea

M. Kahru and R. Elmgren

Title Page

Abstract

Introduction

Conclusions

References

Tables

Figures

◀

▶

◀

▶

Back

Close

Full Screen / Esc

Printer-friendly Version

Interactive Discussion



- Finni, T., Kononen, K., Olsonen, R., and Wallström, K.: The history of cyanobacterial blooms in the Baltic Sea, *Ambio*, 30, 172–178, 2001.
- Gower, J., Hu, C., Borstad, G., and King, S.: Ocean color satellites show extensive lines of floating *Sargassum* in the Gulf of Mexico, *IEEE T. Geosci. Remote*, 44, 3619–3625, 2006.
- 5 Gower, J. F. R., Doerffer, R., and Borstad, G.: Interpretation of the 685 nm peak in water-leaving radiance spectra in terms of fluorescence, absorption and scattering, and its observation by MERIS, *Int. J. Remote Sens.*, 20, 1771–1786, 1999.
- Hajdu, S., Högländer, H., and Larsson, U.: Phytoplankton vertical distributions and composition in Baltic Sea cyanobacterial blooms, *Harmful Algae*, 6, 187–205, 2007.
- 10 Horstmann, U.: Eutrophication and mass occurrence of blue-green algae in the Baltic, *Meren-tutkimuslait, Julk/Havsforskningsinst Skr.*, 239, 83–90, 1975.
- Horstmann, U.: Distribution patterns of temperature and water colour in the Baltic Sea as recorded in satellite images: indicators of plankton growth, *Berichte Institut für Meereskunde Universität Kiel*, 106, 1–147, 1983.
- 15 Hovis, W. A., Clark, D. K., Anderson, F., Austin, R. W., Wilson, W. H., Baker, E. T., Ball, D., Gordon, H. R., Mueller, J. L., El-Sayed, S., Sturm, B., Wrigley, R. C., and Yentsch, C. S.: NIMBUS-7 Coastal Zone Color Scanner: System description and initial imagery, *Science*, 210, 60–63, 1980.
- Hu, C., Feng, L., and Lee, Z.: Uncertainties of SeaWiFS and MODIS remote sensing re-
flectance: implications from clear water measurements, *Remote Sens. Environ.*, 133, 168–
182, 2013.
- 20 Groom, S. B. and Holligan, P. M.: Remote sensing of coccolithophore blooms, *Adv. Space Res.*, 7, 73–78, 1987.
- Kahru, M. and Aitsam, A.: Chlorophyll variability in the Baltic Sea: a pitfall for monitoring, *J. Cons. Int. Explor. Mer.*, 42, 111–115, 1985.
- 25 Kahru, M., Leppänen, J.-M., and Rud, O.: Cyanobacterial blooms cause heating of the sea surface, *Mar. Ecol.-Prog. Ser.*, 101, 1–7, 1993.
- Kahru, M., Horstmann, U., and Rud, O.: Satellite detection of increased cyanobacteria blooms in the Baltic Sea: natural fluctuation or ecosystem change?, *Ambio*, 23, 469–472, 1994.
- 30 Kahru, M.: Using satellites to monitor large-scale environmental change: a case study of cyanobacteria blooms in the Baltic Sea, in: *Monitoring Algal Blooms: New Techniques for Detecting Large-Scale Environmental Change*, edited by: Kahru, M. and Brown, C. W., Springer Verlag Berlin, Heidelberg, New York, 43–61, 1997.

Cyanobacteria accumulations in the Baltic Sea

M. Kahru and R. Elmgren

Title Page

Abstract

Introduction

Conclusions

References

Tables

Figures

◀

▶

◀

▶

Back

Close

Full Screen / Esc

Printer-friendly Version

Interactive Discussion

Kahru, M., Leppänen, J.-M., Rud, O., and Savchuk, O. P.: Cyanobacteria blooms in the Gulf of Finland triggered by saltwater inflow into the Baltic Sea, *Mar. Ecol.-Prog. Ser.*, 207, 13–18, 2000.

Kahru, M., Savchuk, O. P., and Elmgren, R.: Satellite measurements of cyanobacterial bloom frequency in the Baltic Sea: interannual and spatial variability, *Mar. Ecol.-Prog. Ser.*, 343, 15–23, doi:10.3354/meps06943, 2007.

Kidwell, K. B.: NOAA Polar Orbiter Data Users Guide (TIROS-N, NOAA-6, NOAA-7, NOAA-8, NOAA-9, NOAA-10, NOAA-11, NOAA-12, NOAA-14), National Oceanic & Atmospheric Administration, Washington DC, 1995.

Kononen, K.: Dynamics of the toxic cyanobacterial blooms in the Baltic Sea, *Finnish Mar. Res.*, 261, 3–36, 1992.

Kutser, T.: Quantitative detection of chlorophyll in cyanobacterial blooms by satellite remote sensing, *Limnol. Oceanogr.*, 49, 2179–2189, 2004.

Larsson, U., Hajdu, S., Walve, J., and Elmgren, R.: Estimating Baltic nitrogen fixation from the summer increase in upper mixed layer total nitrogen, *Limnol. Oceanogr.*, 46, 811–820, 2001.

Lucke, R. L., Corson, M., McGlothlin, N. R., Butcher, S. D., Wood, D. L., Korwan, D. R., Li, R. R., Snyder, W. A., Davis, C. O., and Chen, D. T.: Hyperspectral Imager for the Coastal Ocean: instrument description and first images, *Appl. Optics*, 50, 11, 1501–1516. 2011.

Matthews, M. W., Bernard, S., and Robertson, L.: An algorithm for detecting trophic status (chlorophyll *a*), cyanobacterial-dominance, surface scums and floating vegetation in inland and coastal waters, *Remote Sens. Environ.*, 124, 637–652, 2012.

Öström, B.: Fertilization of the Baltic by nitrogen-fixation in the blue-green alga *Nodularia spumigena*, *Remote Sens. Environ.*, 4, 305–310, 1976.

Rantajarvi, E.: Alg@line in 2003, 10 years of innovative plankton monitoring and research and operational information service in the Baltic Sea, *Meri – Report Series of the Finnish Institute of Marine Research*, 48, 58 pp., 2003.

Rolff, C., Almesjö, L., and Elmgren, R.: Nitrogen fixation and the abundance of the diazotrophic cyanobacterium *Aphanizomenon* sp. in the Baltic Proper. *Mar. Ecol.-Prog. Ser.*, 332, 107–118, 2007.

Seppälä, J., Ylöstalo, P., Kaitala, S., Hällfors, S., Raateoja, M., and Maunula, P.: Ship-of-opportunity based phycocyanin fluorescence monitoring of the filamentous cyanobacteria bloom dynamics in the Baltic Sea, *Estuar. Coast. Shelf S.*, 73, 489–500, 2007.

Cyanobacteria accumulations in the Baltic Sea

M. Kahru and R. Elmgren

Title Page

Abstract

Introduction

Conclusions

References

Tables

Figures

◀

▶

◀

▶

Back

Close

Full Screen / Esc

Printer-friendly Version

Interactive Discussion



- Simis, S. G. H. and Olsson, J.: Unattended processing of shipborne hyperspectral reflectance measurements, *Remote Sens. Environ.*, 135, 202–212, 2013.
- Simis, S. G. H., Peters, S. W. M., and Gons, H. J.: Remote sensing of the cyanobacterial pigment phycocyanin in turbid inland water, *Limnol. Oceanogr.*, 50, 237–245, 2005.
- 5 Stumpf, R. P. and Frayer, M. L.: Use of AVHRR imagery to examine long-term trends in water clarity in coastal estuaries: example in Florida Bay, in: *Monitoring Algal Blooms: New Techniques for Detecting Large-Scale Environmental Change*, edited by: Kahru, M. and Brown, C. W., Springer Verlag Berlin, Heidelberg, New York, 1–24, 1997.
- Volten, A. H., Haan, J. F. D., Hovenier, J. W., Schreurs, R., Vassen, W., Dekker, A. G., Hoogenboom, J., Charlton, F., and Wouts, R.: Laboratory Measurements of Angular Distributions of Light Scattered by Phytoplankton and Silt, *Limnol. Oceanogr.*, 43, 1180–1197, 1998.
- 10 Walsby, A. E.: Gas vesicles, *Microbiol. Rev.*, 58, 94–144, 1994.
- Wasmund, N.: Occurrence of cyanobacterial blooms in the Baltic Sea in relation to environmental conditions, *Int. Revue Gesamten Hydrobiol.*, 82, 169–184, 1997.
- 15 Wynne, T. T., Stumpf, R. P., Tomlinson, M. C., Warner, R. A., Tester, P. A., Dyble, J., and Fahnenstiel, G. L.: Relating spectral shape to cyanobacterial blooms in the Laurentian Great Lakes, *Int. J. Remote Sens.*, 29, 3665–3672, 2008.

Cyanobacteria accumulations in the Baltic Sea

M. Kahru and R. Elmgren

Table 1. Characteristics of satellite sensors used to detect cyanobacteria accumulations in the Baltic Sea.

Sensor	Satellite	Agency	Spatial resolution, m	Temporal resolution, days	Signal to noise ratio of the red band
MSS	Landsat 2	NASA/USGS	83	18	40
TM	Landsat 5	NASA/USGS	30	16	50
CZCS	Nimbus-7	NASA	825	irregular	110
AVHRR	NOAA-X	NOAA	1100	< 1	3
SeaWiFS	Orbview-2	NASA	1100	~ 2	390
MODIS	Terra	NASA	250/500/1000	~ 2	1000
MODIS	Aqua	NASA	250/500/1000	~ 2	1000
MERIS	ENVISAT	ESA	300/1200	~ 3	883
VIIRS	NPP	NOAA/NASA	370/740	~ 2	750

Title Page

Abstract

Introduction

Conclusions

References

Tables

Figures



Back

Close

Full Screen / Esc

Printer-friendly Version

Interactive Discussion



Cyanobacteria accumulations in the Baltic Sea

M. Kahru and R. Elmgren

Title Page

Abstract

Introduction

Conclusions

References

Tables

Figures



Back

Close

Full Screen / Esc

Printer-friendly Version

Interactive Discussion



Table 2. Number of CZCS scenes over the Baltic Sea available for July–August.

1979	1980	1981	1982	1983	1984	1985
31	64	30	24	39	13	2

Cyanobacteria accumulations in the Baltic Sea

M. Kahru and R. Elmgren

Table 3. Number of AVHRR scenes over the Baltic Sea available for July–August.

1979	1980	1981	1982	1983	1984	1985
33	40	32	37	39	34	46
1986	1987	1988	1989	1990	1991	1992
47	66	68	59	61	62	64
1993	1994	1995	1996	1997	1998	1999
63	76	60	62	108	72	54

Title Page

Abstract

Introduction

Conclusions

References

Tables

Figures



Back

Close

Full Screen / Esc

Printer-friendly Version

Interactive Discussion



BGD

11, 3319–3364, 2014

**Cyanobacteria
accumulations in the
Baltic Sea**

M. Kahru and R. Elmgren

[Title Page](#)[Abstract](#)[Introduction](#)[Conclusions](#)[References](#)[Tables](#)[Figures](#)[Back](#)[Close](#)[Full Screen / Esc](#)[Printer-friendly Version](#)[Interactive Discussion](#)**Table 4.** Number of combined scenes of SeaWiFS, MODIST, MODISA and VIIRS over the Baltic Sea available for July–August.

1998	1999	2000	2001	2002	2003	2004	2005	2006	2007
103	118	240	277	393	450	438	328	320	318
2008	2009	2010	2011	2012	2013				
300	304	307	301	562	617				



Table 5. Number and type of daily detected (“turbid”) and useable (“valid”) satellite datasets, mean fraction of cyanobacteria accumulations (FCA%), total area covered by accumulations (TA) over the Baltic Sea and the sensors used in the analysis.

Year	N of turbid days	N of valid days	FCA%	TA, 1000 km ²	Sensor
1979	17	40	11.2	57	CZCS, AVHRR
1980	23	54	11.7	59	CZCS, AVHRR
1981	17	39	16.8	91	CZCS, AVHRR
1982	21	42	12.9	69	CZCS, AVHRR
1983	27	47	12.3	78	CZCS, AVHRR
1984	13	39	17.0	86	CZCS, AVHRR
1985	9	41	1.1	3	AVHRR
1986	11	47	3.3	14	AVHRR
1987	2	61	0.4	1	AVHRR
1988	7	61	2.1	8	AVHRR
1989	16	56	3.9	23	AVHRR
1990	16	61	3.8	26	AVHRR
1991	19	60	10.2	74	AVHRR
1992	20	60	13.1	60	AVHRR
1993	14	61	6.9	39	AVHRR
1994	21	46	14.3	103	AVHRR
1995	24	60	4.3	40	AVHRR
1996	22	61	2.3	21	AVHRR
1997	35	62	16.0	127	AVHRR
1998	48	62	5.9	129	SeaWiFS, AVHRR
1999	55	62	21.6	209	SeaWiFS, AVHRR
2000	59	62	13.1	178	SeaWiFS, MODIST
2001	55	62	12.4	139	SeaWiFS, MODIST
2002	59	62	14.5	176	SeaWiFS, MODISA, MODIST
2003	59	62	17.9	176	SeaWiFS, MODISA, MODIST
2004	59	62	9.5	155	SeaWiFS, MODISA, MODIST
2005	58	62	25.0	183	MODISA, MODIST
2006	60	62	14.8	174	MODISA, MODIST
2007	56	62	7.1	110	MODISA, MODIST
2008	57	62	25.5	212	MODISA, MODIST
2009	54	62	6.1	160	MODISA, MODIST
2010	55	62	10.7	143	MODISA, MODIST
2011	61	62	16.5	186	MODISA, MODIST
2012	61	62	9.1	155	MODISA, MODIST, VIIRS
2013	62	62	11.1	165	MODISA, MODIST, VIIRS
1979–2013	Total 1252	Total 1990	Mean 11.0	Mean 104	

Cyanobacteria accumulations in the Baltic Sea

M. Kahru and R. Elmgren

Title Page

Abstract

Introduction

Conclusions

References

Tables

Figures



Back

Close

Full Screen / Esc

Printer-friendly Version

Interactive Discussion



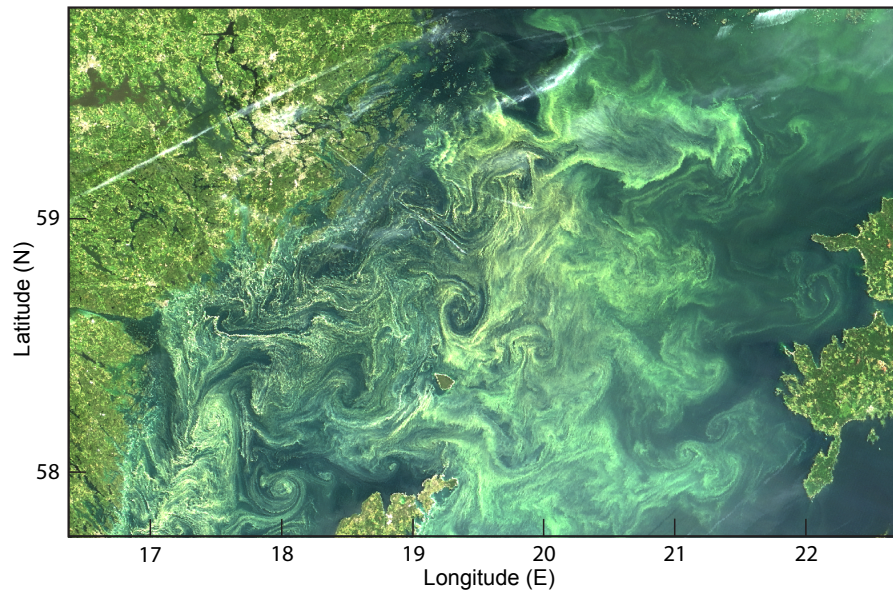


Fig. 1. Cyanobacteria (primarily *Nodularia spumigena*) accumulations in Northern Baltic Proper on 11 July 2005 as shown on MODIS-Terra quasi true color image at 250 m resolution using bands 1 (red), 4 (green), and 3 (blue). Straight white lines are aircraft contrails.

Cyanobacteria accumulations in the Baltic Sea

M. Kahru and R. Elmgren

Title Page

Abstract

Introduction

Conclusions

References

Tables

Figures

◀

▶

◀

▶

Back

Close

Full Screen / Esc

Printer-friendly Version

Interactive Discussion



Cyanobacteria accumulations in the Baltic Sea

M. Kahru and R. Elmgren

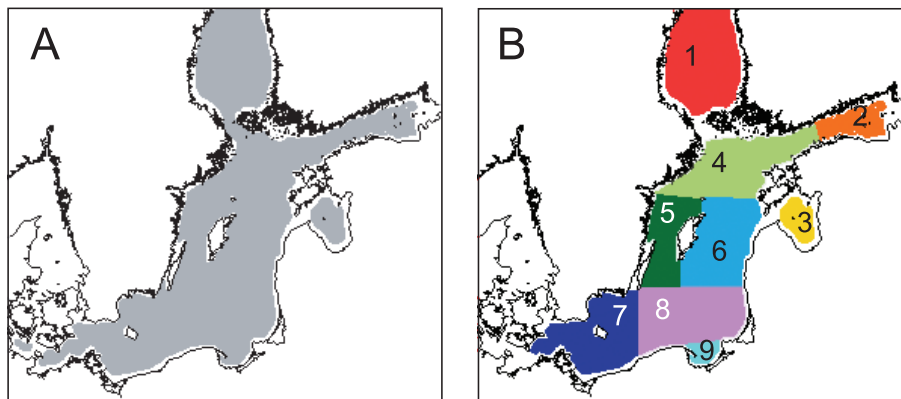


Fig. 2. Study areas in the Baltic Sea. **(A)** The area considered (grey) in mapping cyanobacteria blooms excludes near-shore areas with potentially high turbidity (white, 19.5% of the total sea area). **(B)** Partition into nine 9 separate basins: Bothnian Sea (BS, 1), Gulf of Finland (GF, 2), Gulf of Riga (GR, 3), Northern Baltic Proper (NBP, 4), Western Gotland Basin (WGB, 5), Eastern Gotland Basin (EGB, 6), south-southwestern Baltic Proper (SWBP, 7), south-southeastern Baltic Proper (SEBP, 8), Bay of Gdansk (BG, 9).

[Title Page](#)[Abstract](#)[Introduction](#)[Conclusions](#)[References](#)[Tables](#)[Figures](#)[⏪](#)[⏩](#)[◀](#)[▶](#)[Back](#)[Close](#)[Full Screen / Esc](#)[Printer-friendly Version](#)[Interactive Discussion](#)

Cyanobacteria accumulations in the Baltic Sea

M. Kahru and R. Elmgren

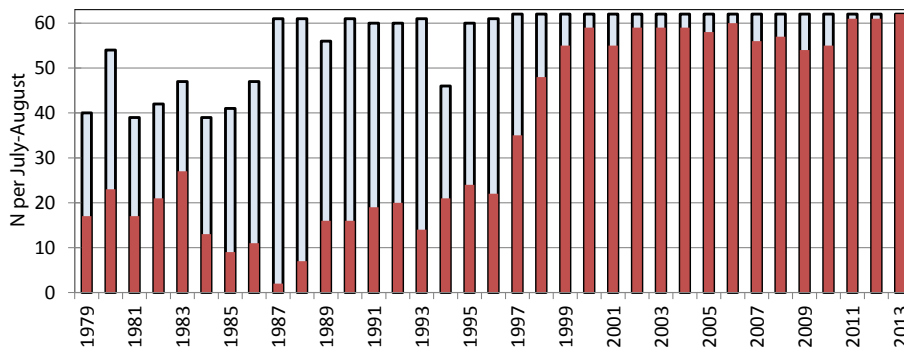


Fig. 3. Number of daily satellite datasets used in the analysis of the July–August season of 1979–2013. Open columns show the total number of daily datasets with valid ocean data, red filled column show the number of daily datasets with detected accumulations.

Title Page

Abstract

Introduction

Conclusions

References

Tables

Figures



Back

Close

Full Screen / Esc

Printer-friendly Version

Interactive Discussion



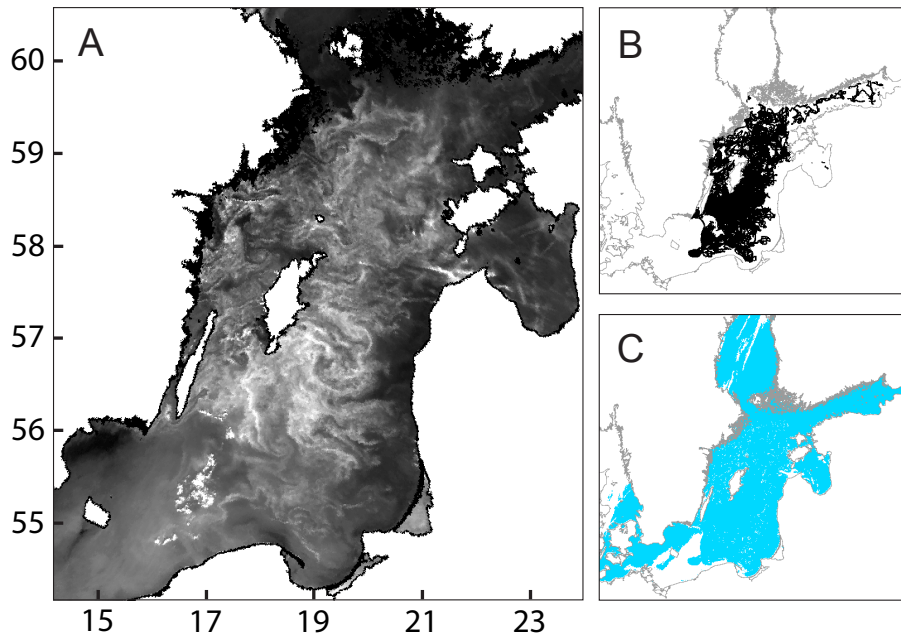


Fig. 4. Example of cyanobacteria detection on AVHRR imagery of central Baltic Sea on 10 July 2005. **(A)** Grayscale image of band 1 albedo (bright tones correspond to higher albedo, dark tones to lower albedo). **(B)** Detected cyanobacteria accumulations (black). **(C)** Valid ocean areas (blue).

Cyanobacteria accumulations in the Baltic Sea

M. Kahru and R. Elmgren

Title Page

Abstract

Introduction

Conclusions

References

Tables

Figures

◀

▶

◀

▶

Back

Close

Full Screen / Esc

Printer-friendly Version

Interactive Discussion



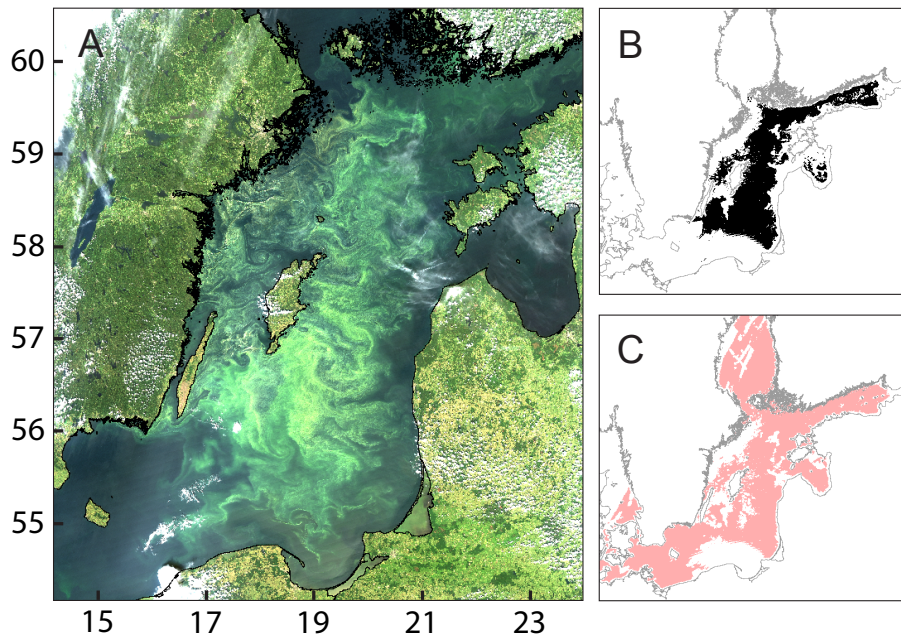


Fig. 5. Example of cyanobacteria detection on MODIS-Aqua imagery of central Baltic Sea on 10 July 2005. **(A)** Quasi true-color image using bands 1 (red), 3 (blue), 4 (green). Small clouds (bright white) can be seen over both land and the sea. **(B)** Detected cyanobacteria accumulations (black). **(C)** Valid ocean areas (pink).

Cyanobacteria accumulations in the Baltic Sea

M. Kahru and R. Elmgren

Title Page

Abstract

Introduction

Conclusions

References

Tables

Figures

◀

▶

◀

▶

Back

Close

Full Screen / Esc

Printer-friendly Version

Interactive Discussion



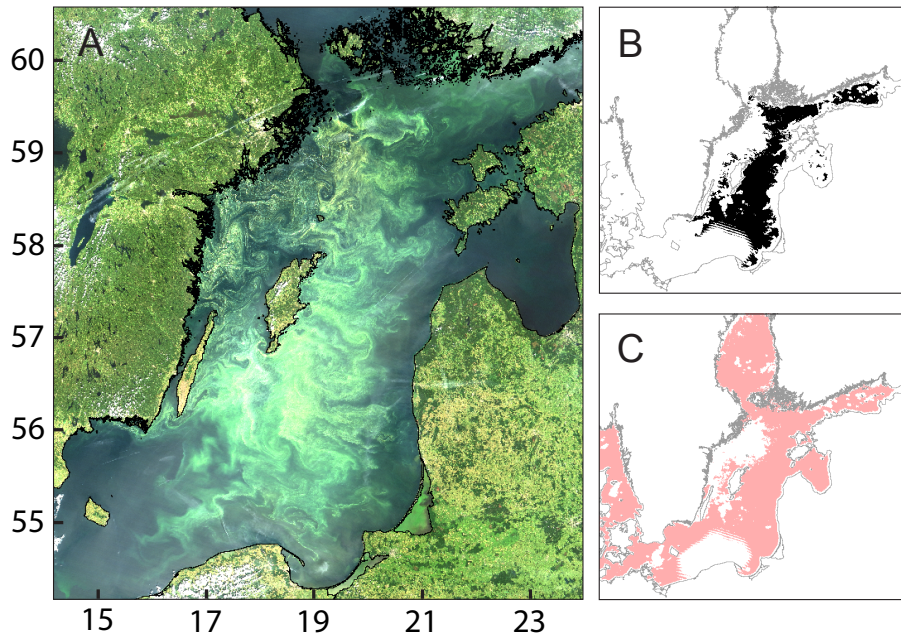


Fig. 6. Example of cyanobacteria detection on MODIS-Terra imagery of central Baltic Sea on 11 July 2005. **(A)** Quasi true-color image using bands 1 (red), 3 (blue), 4 (green). **(B)** Detected cyanobacteria accumulations (black). **(C)** Valid ocean areas (pink).

Cyanobacteria accumulations in the Baltic Sea

M. Kahru and R. Elmgren

Title Page

Abstract

Introduction

Conclusions

References

Tables

Figures

◀

▶

◀

▶

Back

Close

Full Screen / Esc

Printer-friendly Version

Interactive Discussion



Cyanobacteria
accumulations in the
Baltic Sea

M. Kahru and R. Elmgren

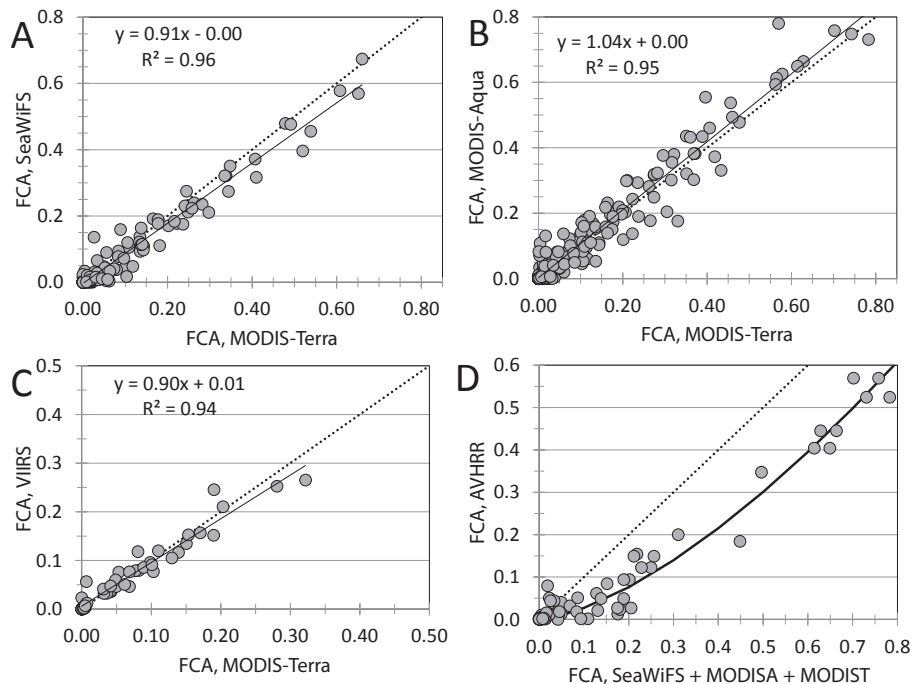


Fig. 7. FCA derived with one sensor vs. FCA derived with another sensor in 9 areas of the Baltic. **(A)** SeaWiFS vs. MODIST, $N = 135$, June–August 2000–2004. **(B)** MODISA vs. MODIST, $N = 243$, June–August 2002–2013. **(C)** VIIRS vs. MODIST, $N = 54$, June–August 2012–2013. **(D)** AVHRR vs. SeaWiFS (1998, 1999), MODISA (2005) and MODIST (2000, 2005), $N = 108$. Dotted line is the one-to-one line and solid line is the estimated linear regression line. For AVHRR the power function $FCA_N = 0.85 \times FCA^{1.5}$ was used to convert FCA_N to FCA.

Title Page

Abstract

Introduction

Conclusions

References

Tables

Figures



Back

Close

Full Screen / Esc

Printer-friendly Version

Interactive Discussion



Cyanobacteria accumulations in the Baltic Sea

M. Kahru and R. Elmgren

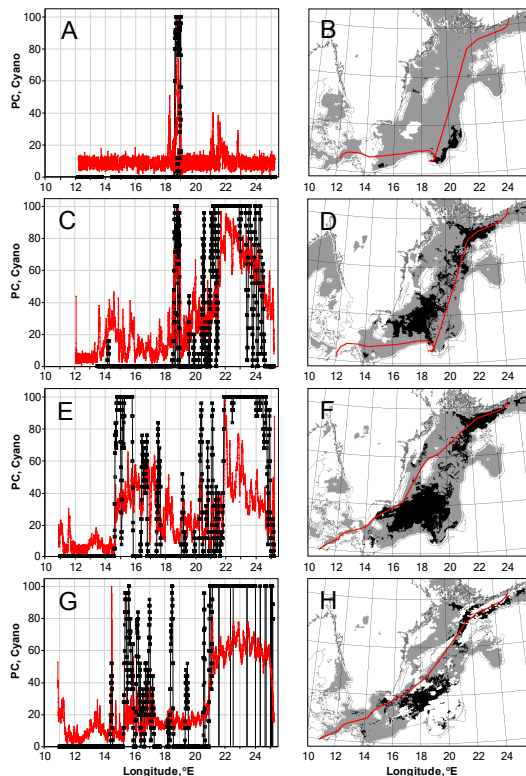


Fig. 8. Comparison between ship transects of phycocyanin (PC) fluorescence (left panels) and satellite detection of cyanobacteria accumulations (right panels) in July 2010. Along-transect PC fluorescence (red, relative scale from 0 to 100) is shown together with the corresponding satellite mean score for accumulations in the 5×5 pixel window centered at the nearest pixel (black squares). Satellite maps show detected accumulations (black), valid areas with no detected accumulations (gray), missing data due to clouds (white) and the ship track (red line). (A, B) – 3 July; (C, D) – 10 July; (E, F) – 12 July; (G, H) – 20 July.

[Title Page](#)
[Abstract](#)
[Introduction](#)
[Conclusions](#)
[References](#)
[Tables](#)
[Figures](#)
[◀](#)
[▶](#)
[◀](#)
[▶](#)
[Back](#)
[Close](#)
[Full Screen / Esc](#)
[Printer-friendly Version](#)
[Interactive Discussion](#)

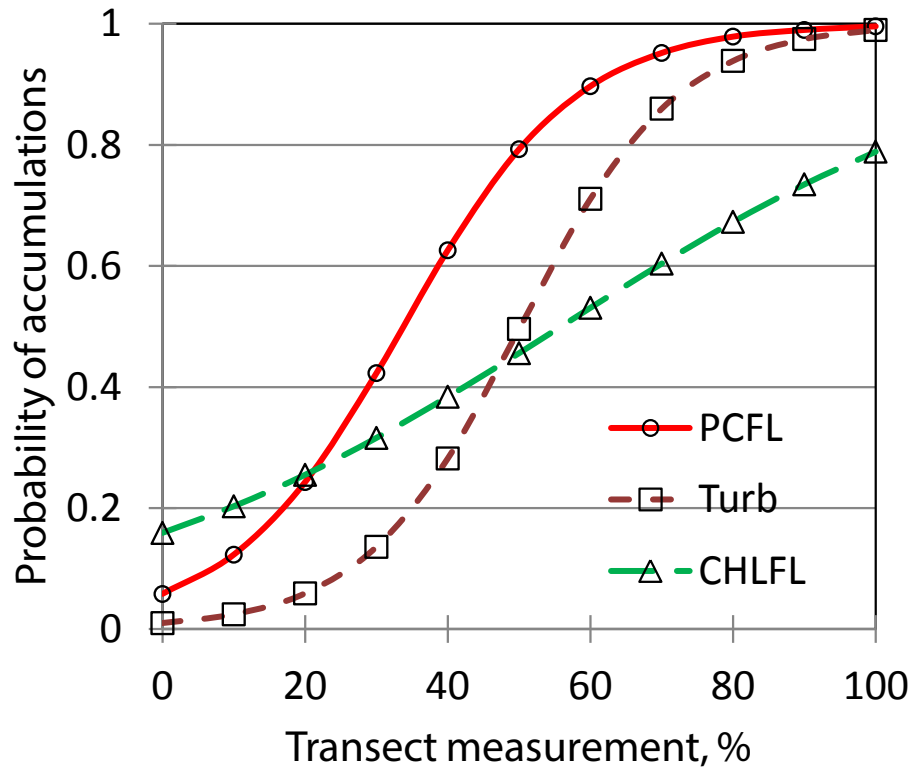



Fig. 9. Probability of surface cyanobacteria accumulations estimated with the logistic regression as a function of phycocyanin fluorescence (PCFL), turbidity (Turb) and Chla fluorescence (CHLFL) at approximately 5 m depth. The values of PCFL, Turb and CHLFL are normalized to a scale from 0 to to 100.

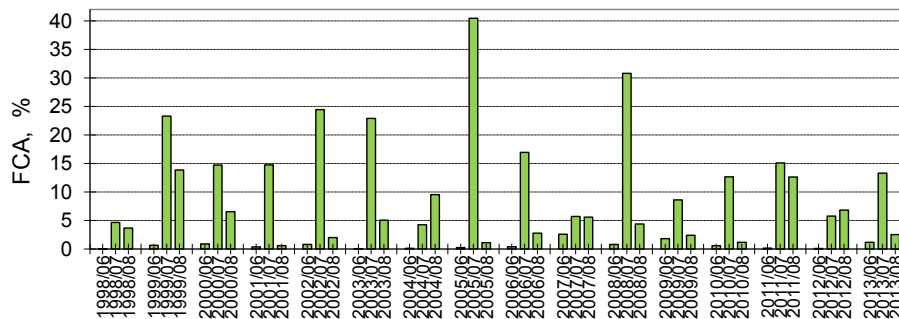


Fig. 10. Monthly mean FCA in June-July-August for the Baltic Sea based on ocean color satellite data in 1998–2013.

Cyanobacteria accumulations in the Baltic Sea

M. Kahru and R. Elmgren

[Title Page](#)

[Abstract](#) [Introduction](#)

[Conclusions](#) [References](#)

[Tables](#) [Figures](#)

[◀](#) [▶](#)

[◀](#) [▶](#)

[Back](#) [Close](#)

[Full Screen / Esc](#)

[Printer-friendly Version](#)

[Interactive Discussion](#)



Cyanobacteria accumulations in the Baltic Sea

M. Kahru and R. Elmgren

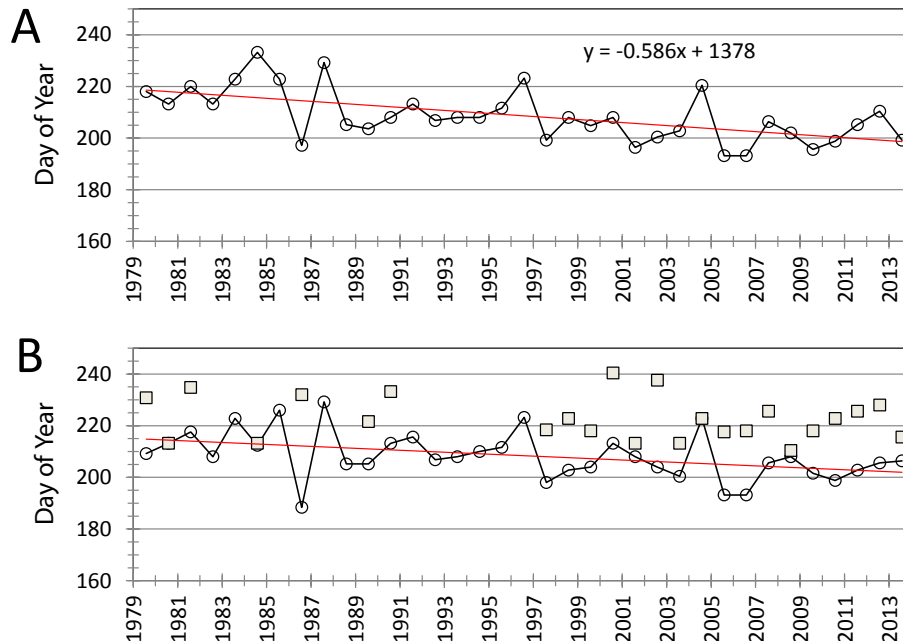


Fig. 11. Temporal changes in the center of timing of the occurrence of cyanobacteria accumulations (median of the area). **(A)** the whole Baltic Sea; **(B)** Northern Baltic Proper (circles connected by solid black line) and Bothnian Sea (gray squares). Red line is the estimated linear regression for the whole Baltic **(A)** or the Northern Baltic Proper **(B)**. 1 July is year day 182 (year day 183 on leap years), year day 200 is 18 July (19 July on leap year).

[Title Page](#)
[Abstract](#)
[Introduction](#)
[Conclusions](#)
[References](#)
[Tables](#)
[Figures](#)
[◀](#)
[▶](#)
[◀](#)
[▶](#)
[Back](#)
[Close](#)
[Full Screen / Esc](#)
[Printer-friendly Version](#)
[Interactive Discussion](#)


Cyanobacteria accumulations in the Baltic Sea

M. Kahru and R. Elmgren

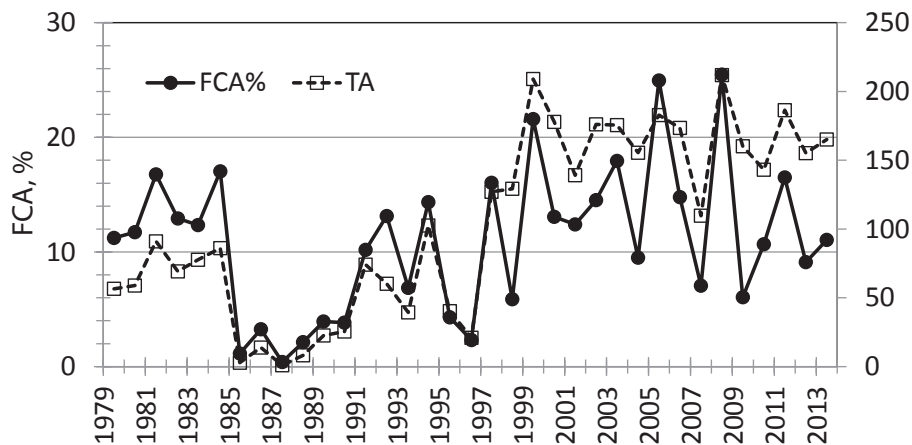


Fig. 12. Mean FCA (%) for the July–August period in the Baltic Sea (solid black circle, left axis) and the corresponding total area (TA, km²; rectangle, dashed line) of the accumulations (corresponding numerical data in Table 5).

Title Page

Abstract

Introduction

Conclusions

References

Tables

Figures

◀

▶

◀

▶

Back

Close

Full Screen / Esc

Printer-friendly Version

Interactive Discussion



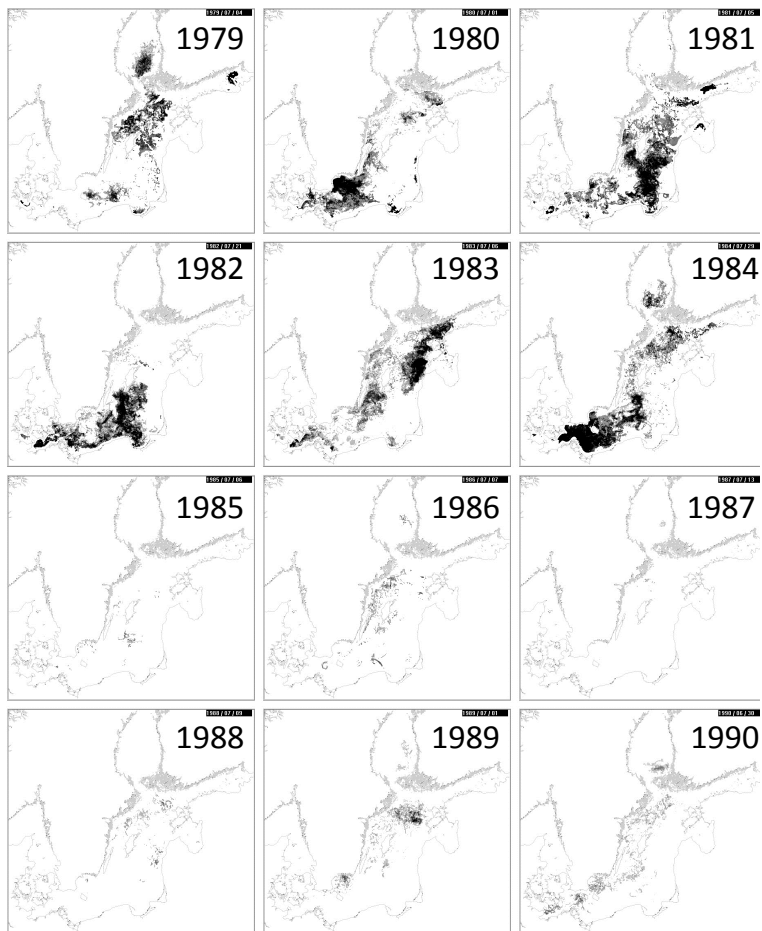


Fig. 13a. Maps of the mean July–August FCA in the Baltic Sea. Gray-scale from light to dark corresponds to increasing FCA. **(A)** 1979–1990. **(B)** 1991–2002. **(C)** 2003–2013.

Cyanobacteria accumulations in the Baltic Sea

M. Kahru and R. Elmgren

Title Page

Abstract

Introduction

Conclusions

References

Tables

Figures

◀

▶

◀

▶

Back

Close

Full Screen / Esc

Printer-friendly Version

Interactive Discussion



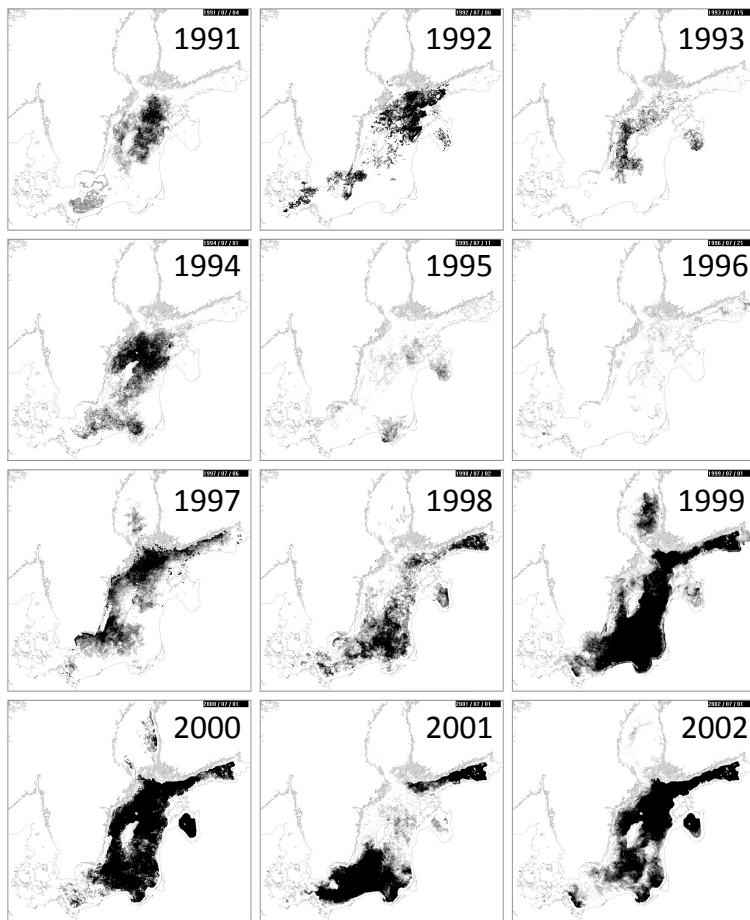


Fig. 13b. Continued.

Cyanobacteria accumulations in the Baltic Sea

M. Kahru and R. Elmgren

Title Page

Abstract Introduction

Conclusions References

Tables Figures

◀ ▶

◀ ▶

Back Close

Full Screen / Esc

Printer-friendly Version

Interactive Discussion



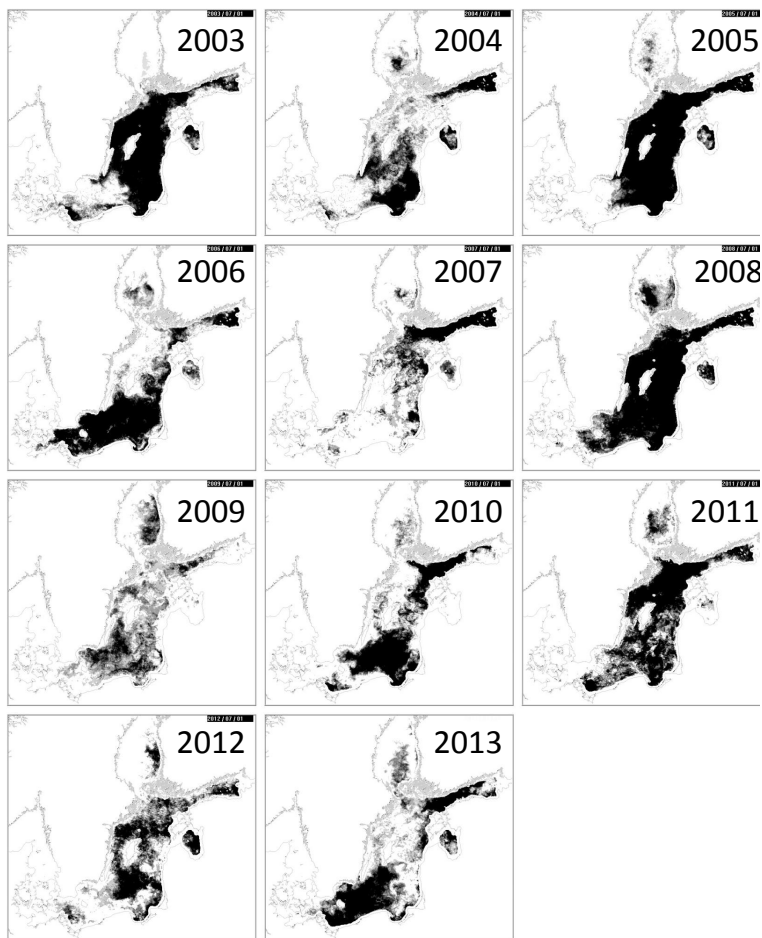


Fig. 13c. Continued.

Cyanobacteria accumulations in the Baltic Sea

M. Kahru and R. Elmgren

Title Page

Abstract

Introduction

Conclusions

References

Tables

Figures

◀

▶

◀

▶

Back

Close

Full Screen / Esc

Printer-friendly Version

Interactive Discussion



Cyanobacteria accumulations in the Baltic Sea

M. Kahru and R. Elmgren

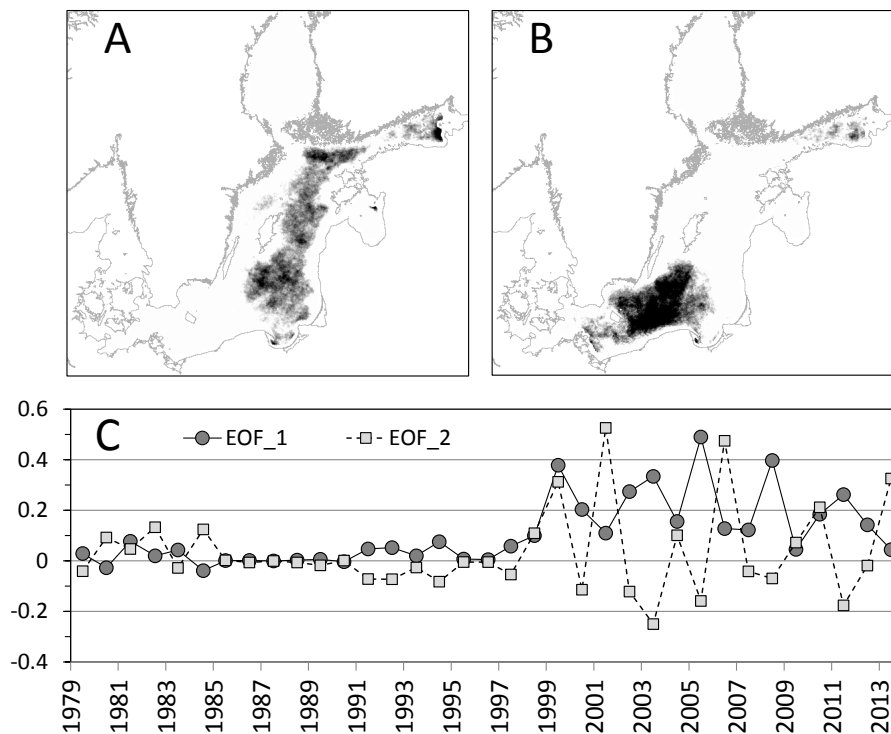


Fig. 14. Dominant distribution patterns, i.e. empirical orthogonal functions EOF 1 (**A**) and EOF 2 (**B**) of the annual July–August FCA in the Baltic Sea for 1979–2013 and their temporal loadings (**C**).

Cyanobacteria accumulations in the Baltic Sea

M. Kahru and R. Elmgren

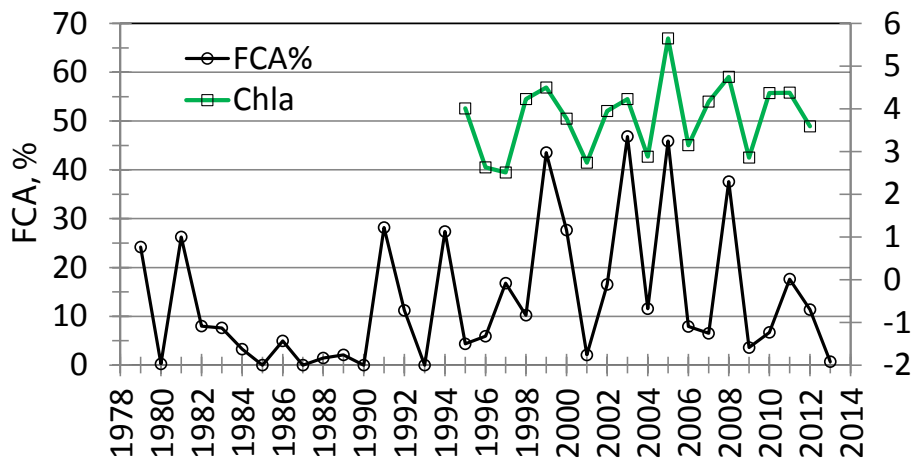


Fig. 15. Time series from along Algaline ship transects in the Eastern Gotland basin in July–August: mean extracted chlorophyll *a* at approximately 5 m depth (green line, right axis) and the corresponding frequency of cyanobacteria accumulations (black line, left axis).

Title Page

Abstract

Introduction

Conclusions

References

Tables

Figures

◀

▶

◀

▶

Back

Close

Full Screen / Esc

Printer-friendly Version

Interactive Discussion

